Electrochemistry Communications 163 (2024) 107736

Contents lists available at ScienceDirect

Electrochemistry Communications

journal homepage: www.elsevier.com/locate/elecom

Full Communication

Detection of electrocatalytical and -chemical processes by means of in situ flow NMR spectroscopy

Anastasia Vyalikh [a,b,*], Wolfram Münchgesang [b,c], Juan-Jesús Velasco-Vélez [d,e,f]

[a] Institut für Festkörper- und Materialphysik, Technische Universität Dresden, 01062 Dresden, Germany
[b] Institut für Experimentelle Physik, Technische Universität Bergakademie Freiberg, 09599 Freiberg, Germany
[c] Fraunhofer Institute for Wind Energy System IWES, Am Haupttor 4310, 06237 Leuna, Germany
[d] Max Planck Institute for Chemical Energy Conversion, Mülheim an der Ruhr 45470, Germany
[e] Fritz-Haber-Institut der Max-Planck-Gesellschaft, Berlin 14195, Germany
[f] ALBA Synchrotron Light Source, Cerdanyola del Vallès, Barcelona 08290, Spain

ARTICLE INFO

Keywords:
In situ NMR
Flow NMR
Copper electrodeposition
Electroreduction
CO_2

ABSTRACT

In situ studies of electrochemical processes using NMR offer valuable information on reaction mechanisms, kinetics, and species identification, making it a powerful tool in electrochemistry research. In this study, we present the design of an in situ redox-flow NMR cell that allows for a continuous flow of liquid (electrolyte) or gas, application of electrical voltage, and recording of NMR signals. The utility of this setup is demonstrated through two case studies: electrochemical copper deposition on a gold electrode and the electrochemical conversion of carbon dioxide into hydrocarbon products. Specifically, the presence of multicarbon products containing C–C bonds generated during the electrochemical reduction reaction is confirmed in the ^{2}H NMR spectra in the latter example. These findings highlight the ability of the in situ redox-flow NMR cell to directly monitor reaction intermediates and products, thereby enabling the elucidation of reaction mechanisms for the efficient and selective production of valuable hydrocarbon products through the conversion of CO_2 into value-added chemicals. In contrast to other reported in situ NMR cells, the presented cell is suitable for multiple uses, and allows detecting NMR signals not only from exhaust products but also from those formed on the catalyst surface.

1. Introduction

Currently, renewable energies are replacing fossil chemicals and fossil fuels. However, wind, water and solar power are not continuously available meaning the supply of energy is less stable compared to large power stations. To deal with excess energy produced during peaks in solar and wind power production, storage solutions, which make energy continuously available and cost-effective are required. New storage concepts include power-to-X technologies based on diverse conversion mechanisms to energy carriers like gas, liquids and chemicals [1,2]. Upon the power-to-chemicals conversion pathway, energy is stored in the form of chemical bonds in reaction products. It is known that a large amount of energy is stored in covalent bonds of hydrocarbon molecules offering the hydrocarbon resources to be the largest energy sources in the world.

Over the last decade, there has been an increasing interest in the use of carbon dioxide (CO_2) as a resource to produce sustainable liquid hydrocarbon fuels [3–5]. The concentration of CO_2 in the atmosphere has raised remarkably due to burning of carbon-rich fossil fuels leading to the "greenhouse effect". From the perspective of mitigating climate change, CO_2 capture and utilization can be an important environmental and economic incentive [6]. Thus, the direct electrochemical reduction of captured CO_2 to functional molecules is therefore of high relevance [7]. However, C_1 products (single-carbon molecules) resulting from the CO_2 hydrogenation are highly volatile and therefore extremely flammable [8]. The generation of multicarbon products containing C–C bonds (denoted frequently as C_{2+} products) is beneficial for the synthesis of long-chain hydrocarbon fuels and for providing more complex feedstock for chemicals production. The current research efforts have been focused on identifying key reaction intermediates and establishing the mechanisms for the selective CO_2 conversion towards a desired product [7,9–12]. To improve efficiency of such conversion, experimental techniques, which allow characterization and diagnosis on the different time and length scales, are needed.

* Corresponding author at: Institut für Festkörper- und Materialphysik, Technische Universität Dresden, 01062 Dresden, Germany.
E-mail address: anastasia.vyalikh@tu-dresden.de (A. Vyalikh).

https://doi.org/10.1016/j.elecom.2024.107736
Received 16 April 2024; Received in revised form 23 April 2024; Accepted 24 April 2024
Available online 25 April 2024

The use of ex situ characterisation of electrochemical reactions might result in incomplete information regarding an understanding of overall processes, because various metastable, intermediate, and/or short-lived phases exist only at a certain electrochemical potential. Thus, the application of a non-invasive analysis tool that can follow the reactions in situ or operando and provide real time information on the dynamic structural changes and processes is therefore highly desired.

Nuclear magnetic resonance (NMR) spectroscopy offers unique possibilities for studying both the structure and mobility in various media, including gases, liquids, crystalline and amorphous solids. In contrast to other analytical methods, NMR affords quantitative identification of various chemical species in a system. Such advantages of NMR as well as its noninvasiveness promote this technique to be used for in situ studies of electrochemical or electrocatalytical processes [13,14]. State-of-the-art experimental designs and performance improvements in the field of electrochemistry coupled with NMR spectroscopy have been reviewed in Ref. [15]. The in situ NMR cell assemblies commonly represent either electrodes placed in a standard 5 mm or 10 mm NMR sample tube [16,17] or sealed Bellcore's plastic bag cells inserted into a solenoid NMR detection coil [18,19]. However, despite the unique merits of in situ NMR spectroscopy, the optimal performance is limited either by the NMR technical shortcomings (interference of the magnetic field of the magnet and the cell current, loss of the magnetic field homogeneity and NMR coil size limits) or the cell design (electrochemical stability and necessity to release excessive gas overpressure as a result of electrochemical reaction in a plastic bag cell). There have been further efforts towards the optimal performance of in situ NMR, such as to reduce interference of the electrodes with local magnetic fields by modifying the electrode surface [20] and to increase an accuracy of the quantitative determination [21]. The technical implementation of in situ NMR becomes even more challenging in the fuel cell research, which requires in addition the pathways of fuel, oxidant, and exhaust. Hwang and Han proposed to use a toroid cavity detector in order to analyse simultaneously the exhausts of the anode and cathode in the direct methanol fuel cell [22].

Previously, we optimized design of the electrochemical cell in such a way, that it enabled detection of NMR signals with high sensitivity thereby retaining the efficient battery performance and cyclability [23,24]. In the present work, we demonstrate the design of a redox-flow cell allowing its application for in situ NMR spectroscopy of electrochemical or electrocatalytical processes. Such setup has been developed to directly monitor the structural changes in electrolyte and on catalytically active electrode, as well as to identify and quantify the products formed as a result of electrochemical or electrocatalytical reaction within the redox-flow cell. The combined functionality of this cell enables a continuous flow of liquid (electrolyte) or gas preventing depletion of ions and changes in the electrolyte concentration, while varying the applied voltage and recording NMR signals under operating conditions. In contrast to the cell designs reported in literature, the presented in this work redox-flow cell has been developed for the multiple use, and offers the monitoring of reaction intermediates and products on the catalyst. The performance of this setup is demonstrated using two examples – electrochemical copper deposition on a gold electrode and electrochemical conversion of carbon dioxide into hydrocarbon products.

2. Materials and methods

2.1. Design of the redox-flow cell and in-situ NMR setup

The cylindrical redox-flow cell of the length of 36 mm and the outer diameter of 8 mm is made of polyether ether ketone (PEEK), which is an electrical insulator and chemically inert. The end faces of the cell cylinder have inlet and outlet openings for supplying and removing gas and liquid to/from the cell. Ethylene tetrafluoroethylene (ETFE) tubing is used to connect the cell inlet and outlet to a diaphragm dosing pump (SIMDOS® 02/10, KNF Neuberger GmbH, Germany). Metal wires passing through the end faces of the cell cylinder are used for connecting three electrodes to the NMR probehead. The loaded cells were hermetically sealed from outside by a PEEK housing and Viton O-rings. To provide mechanical stability and prevent potential leaks, the wires were secured to the housing using epoxy adhesive. For NMR measurements, the redox-flow cell was placed in an 8 mm radio-frequency solenoid coil of the NMR probehead so that NMR signals can be measured at operando conditions (Fig. 1). The electrical contacts of the probehead were connected to a potentiostat (Ivium CompactStat, Ivium Technologies B.V., Eindhoven, The Netherlands).

2.2. NMR measurements

NMR measurements were performed on a Bruker Avance III 400 MHz spectrometer using a static in situ probehead (NMR Service GmbH, Erfurt, Germany). A silver radio-frequency solenoid coil was used to minimize the contribution to ^{63}Cu NMR from the experimental setup. ^{63}Cu and ^{2}H NMR spectra were recorded using a 90°- pulse sequence. For ^{63}Cu spectra a single 90°-pulse of 4 μs pulse duration, a recycle delay of 1 s, a spectral window of 625 kHz and 1024 repetitions were used. For ^{2}H spectra a single 90°-pulse of 6 μs pulse duration, a recycle delay of 3 s, a spectral window of 6.25 kHz and 16 and 32 repetitions were applied. In addition, ^{2}H solid-echo spectra (90°-τ-90°-τ-acquision) with an echo delay τ of 60 μs were acquired. Prior to Fourier transformation the exponential multiplication with 30–Hz line broadening was applied. ^{2}H spectra were calibrated using the external reference of D_2O (at 4.8 ppm) measured in the custom made cylindrical PEEK container. ^{63}Cu chemical shift was calibrated to pure metallic Cu at 0 ppm by measuring metallic copper mesh and wire and subtracting the probehead background. The resonance shift of metallic Cu is 2350 ppm in respect to a reference ^{63}Cu signal in CuCl caused by spin polarisation of the conduction electrons (Knight shift) [25]. All measurements were performed at room temperature.

2.3. Experimental details for Cu electrodeposition

Gold and platinum plates, each with a thickness of 0.1 mm (99.99 %, Chempure, Karlsruhe, Germany) were used as the working (WE) and reference (RE) electrodes. Gold and platinum wires were spot welded to the plates for electrical connection purposes. A counter electrode (CE) consisting of a platinum wire was included to complete the cell. The 5 mM $CuSO_4$ aqueous electrolyte was prepared by diluting 0.798 g of $CuSO_4$ (Sigma Aldrich, anhydrous powder, 99.99 %) in 1 L of Milli-Q water (18.2 MΩ) at room temperature. ^{2}H isotope enriched water (D_2O) was used in order to acquire background-free spectra. The electrolyte was continuously saturated with pure N_2 gas by bubbling for eliminating dissolved gases.

Chronoamperometry was used to deposit copper on a gold electrode. Firstly, the cell voltage is stepped down with an interval of 0.25 V from open circuit voltage (0 V) to –1.25 V vs Pt, then increased to + 1 V. At each potential value subsequently ^{63}Cu and ^{2}H NMR spectra were measured, while cell current was quenched during the application of rf-pulses to reduce noise in the spectra. For a retuning a resonance frequency from ^{63}Cu and ^{2}H and back, an automatic Tuning/Matching controller (NMR Service GmbH, Erfurt, Germany) was used. As the next step, –2 V vs Pt was applied during 40 min yielding an over-potential deposition of copper. ^{63}Cu NMR spectra were measured at different time intervals.

2.4. Experimental details for electrochemical reduction of carbon dioxide

In the first step, the copper electrode was prepared outside the redox-flow cell in a classic beaker set-up by electrodeposition. The electrode was deposited from 5 mM $CuSO_4$ on a gold plate at an electrical potential of −2 V vs Pt for one hour using chronoamperometry, following an

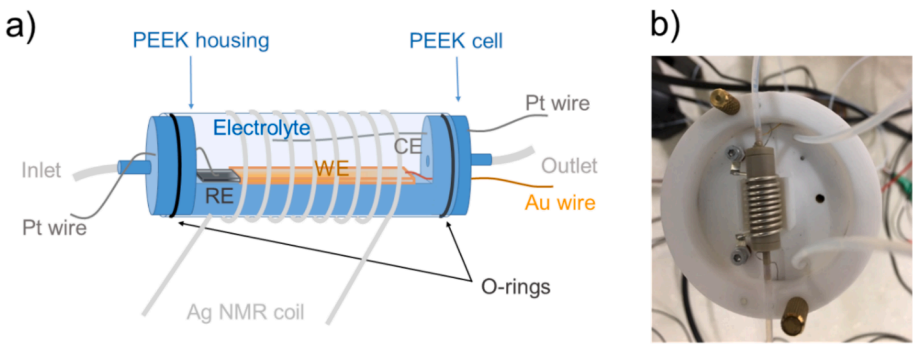

Fig. 1. (a) Schematic drawing of the redox-flow cell inserted in a solenoid NMR coil, where WE is a gold plate working electrode, CE is a platinum wire counter electrode, and RE is a platinum plate reference electrode. (b) In-situ NMR probehead with a redox-flow cell (top view).

approach described in a study that utilized in situ X-ray absorption electrochemical cells [26,27]. The copper film coated electrode was placed into the redox-flow cell and fixed. The electrolyte was prepared using a 100 mM $KHCO_3$ (Grüssing GmbH, Filsum, Germany) solution in a H_2O/D_2O (1:2) mixture (pH 6.8) and pumped through the electrochemical redox-flow cell at a constant flow rate of 1 ml/min. Prior to the measurement, the electrolyte was bubbled with CO_2 for 30 min to remove oxygen in the solution and saturate the solution.

A platinum wire and platinum foil of 0.1 mm thickness were used as CE and RE, respectively. Chronoamperometry was used as an electrochemical method. The cell voltage is stepped down from open circuit voltage to −1 V, then up to + 1 V, and finally down to 0 V vs Pt. During the chronoamperometry experiment of a total duration of 65 min, 64 ^{2}H NMR spectra were measured. The spectra were recorded each 50 s using a continuous potential variation rate of 0.075 V/s yielding a potential resolution of 0.01 V. The reaction products were analysed by fitting 1D ^{2}H NMR spectra using DMFit [28].

3. Results and discussion

3.1. Electrodeposition of Cu from $CuSO_4$ aqueous electrolyte on a gold electrode

Catalytically active surface plays an important role in electrocatalytical processes. For example, for electrochemical reduction of carbon dioxide, various valuable hydrocarbons such as methane, ethane, ethanol, or n-propanol can be formed depending on the catalyst's surface and electrocatalytical operating conditions [29–34]. In this work, we attempt to observe the process of electrochemical deposition of Cu from a solution using NMR spectroscopy. Cu is one of very few materials capable of converting CO_2 to C_{2+} products with significant efficiencies [35]. NMR can enable the quantification of structural changes with respect to the electrochemical treatment, once their spectral signatures appear at different states of charge [23]. Here we use $CuSO_4$ aqueous solution as a source of Cu ions for preparing Cu thin film electrode. Electrolyte solution is fed continuously into the redox-flow cell containing a gold foil used as WE for copper electrodeposition, while electrical signal is applied to the electrodes. Probing the NMR-active ^{63}Cu isotopes, the spectral changes, such as an increase of ^{63}Cu NMR intensity or an appearance of new signals associated with Cu film preparation can be observed. In addition, ^{2}H NMR spectra measured consequently at each potential value allow for monitoring the structural changes occurring during the electrodeposition process, such as generation of reaction intermediates in electrolyte or metal hydroxides on the electrode surface.

The two-dimensional (2D) spectra in Fig. 2a and 2b allow visualization of the ^{63}Cu and ^{2}H spectral intensity, respectively, as a function of applied voltage indicated on the top of Fig. 2a. Each 2D spectrum is a set of the 1D NMR spectra obtained at different time intervals after applying a potential. The chemical shift scales are indicated in vertical direction

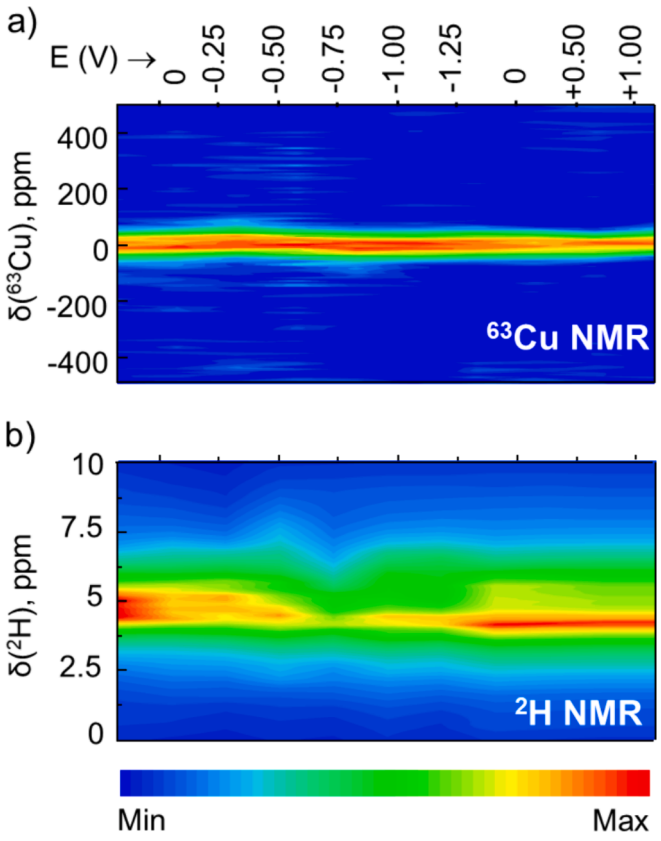

Fig. 2. Two-dimensional (a) ^{63}Cu and (b) ^{2}H NMR spectra as a function of applied potential. The intensity scale is shown as a colour bar underneath the spectra.

in Fig. 2a and 2b.

The starting ^{63}Cu NMR spectrum of the redox-flow cell measured at open circuit voltage shows a single broad nearly symmetrical signal around 0 ppm. This signal is attributed to metallic copper present in the NMR probehead and to copper ions from sulphate solution flowing through the cell. When the potential is applied and varied from 0 V to −1.25 V and to + 1 V, no ^{63}Cu NMR spectral changes within the signal-to-noise ratio of these measurements have been observed (Fig. 2a).

In contrast, the 2D ^{2}H NMR spectrum of the same system demonstrates the visible changes as the different potential values are applied (Fig. 2b). The starting ^{2}H NMR spectrum measured at open circuit voltage shows a complex spectral profile in the range between 4 to 6 ppm. The signals in this range are attributed to the different water arrangements, such as highly mobile bulk water, water molecules from

hydration shells around Cu^{2+} and SO_4^{2-} ions and water molecules near the electrode surface screened by the conductive layer. When the negative voltage is applied, the spectral profile changes, revealing a decrease in ^2H signal intensity in this spectral range and the appearance of a broad signal near 7 ppm, whose assignment is impossible based on the present data. This can be explained by consumption of water for the formation of reaction intermediates. At −0.75 V the total spectral intensity is minimal indicating that a significant part of ^2H becomes invisible for NMR. Commonly, drop out of the NMR intensity can be caused by the presence of paramagnetic species, or dynamic exchange on the NMR time scale, or the relaxation effects resulting in line broadening in NMR spectra of solids. Indeed, the generation of radical intermediates, such as hydroxyl radicals, which exhibit paramagnetism, is known to occur in an electrochemical reaction [36]. The scenario of chemical exchange, when exchanging resonances broaden and merge, resulting in a poorly visible spectrum, could be evidenced by heating or cooling the system. This would disrupt the electrochemical conditions and consequently affect the observed data. Furthermore, it is rather difficult to believe that various molecular species present in our system at a specific potential have identical intermediate exchange rates and would simultaneously enter a coalescence regime at a given temperature. The relaxation effects can be justified by measuring echo spectra, which are sensitive to motional changes in a spin system. As the echo spectra (not shown here) revealed only an insignificant difference with those measured by the one-pulse sequence, we excluded the relaxation effects to explain the intensity drop out. At the lower voltage values, the intensity increase of the dominant signals and an appearance of new signals in a low-field region (around 6 ppm) are observed. This can be explained by the fact that under continuous water and electrolyte supply, the highly reactive water radical intermediates oxidize and produce other ^2H-containing molecules, which contribute now to the spectral intensity.

Thus, the intermediate conclusion is that within the applied potential window, no visible changes are found in the ^{63}Cu NMR data, while ^2H NMR allows to detect the spectral changes in the system under study. Although, a small amount of ^{63}Cu species could be adsorbed from electrolyte onto the electrode surface, their detection is restricted due to a low receptivity of ^{63}Cu NMR. A higher concentration of ^2H in the system and a higher mobility of solvent molecules, which results in a motional averaging of NMR lines, provide stronger visualization effect in the ^2H NMR spectra.

As the next, the potential of −2 V vs Pt has been continuously applied and the ^{63}Cu NMR spectra have been measured after 5, 10, and 35 min as indicated in Fig. 3a. The integrated ^{63}Cu spectral intensities are plotted in Fig. 3b revealing the increase of the intensity with deposition time and hence the growth of Cu concentration within the cell. This finding is attributed to metallic Cu deposition onto the gold electrode surface. The minor intensity at ca. −500 ppm after 35 min deposition points out to other Cu phases perhaps formed on the gold surface, such as CuH and CuOH. No other signals in the wide spectral window of 625 kHz, which can comprise the resonances affected by diamagnetic and paramagnetic shielding and by strong quadrupolar interactions [37,38], have been observed. After the cell disassembling the formation of metallic red colored film on the electrode attributed to Cu deposition was observed.

3.2. Electrochemical reduction of CO_2

In following, the redox-flow NMR cell is used for real time detection of the reaction intermediates in the course of electrochemical reduction of CO_2. As catalytically active surface, metallic copper film prepared in the same way as in the previous section is used. Electrolyte with a dissolved CO_2 gas is fed through the redox-flow cell when the potential is applied. The results have been evaluated with respect to the highest output and particular selectivity of the desired multicarbon products.

The ^2H one-pulse NMR spectra measured in the course of an electrochemical reaction are presented as a two-dimensional spectrum in

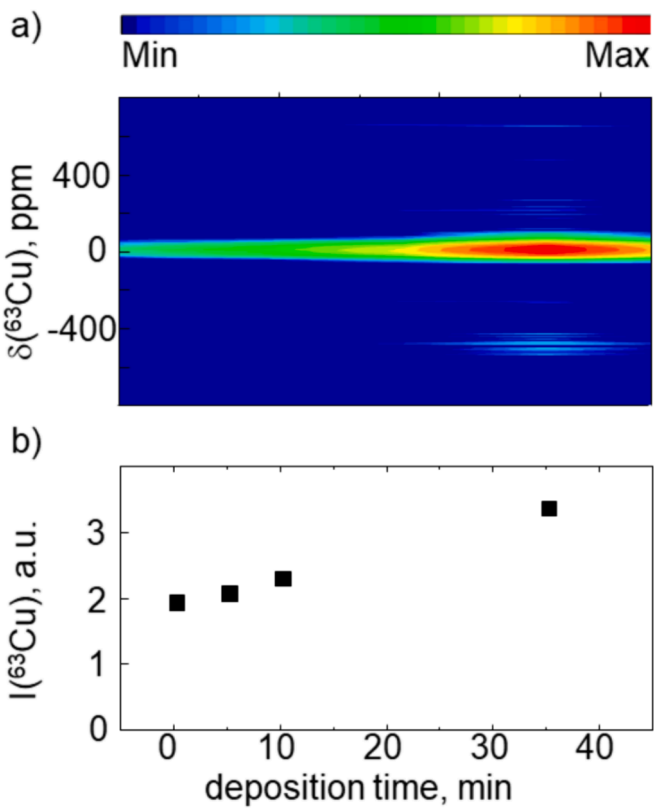

Fig. 3. (a) Two-dimensional ^{63}Cu NMR spectrum as a function of deposition time at a voltage of –2 V. (b) The intensity scale is shown as a colour bar above the spectrum. Intensity of ^{63}Cu NMR signal as a function of deposition time.

Fig. 4a, where the ^2H chemical shift (horizontal direction) is plotted against the reaction time (vertical direction). The time dependence of the applied electrode potential and the transient current behaviour resulting from a voltage step are shown in Fig. 4b and 4c, respectively. One can see that the observed current density deviates from the expected trend with applied potential. This discrepancy has been explained by the restricted charge transport to WE due to the geometric constriction of the present cell design, which is associated with the following factors: First, the WE area is much larger than that of CE. Second, there are charge transport limitations from electrolyte to electrode surface. The ^2H spectra in Fig. 4a are dominated by a complex asymmetric broad line centered at 4.6 ppm, those profile and intensity changes with applied potential. This evidences chemical changes and an appearance of reaction intermediates and products in the course of electrochemical reduction of CO_2. However, to identify key reaction intermediates for specific products and establish the reaction mechanism, quantitative analysis of each 1D NMR spectrum is required. Due to complexity of the electrochemical system and line overlapping in the NMR spectra, unambiguous fit of the data that would enable accurate quantitative analysis is not possible. In the present work, we focus on demonstrating the feasibility of the in situ NMR approach and analyse qualitatively the selected spectra towards the structural information. The slices selected from the 2D spectrum are labeled by the dotted lines and numbered from N1 to N9 (Fig. 4a) and stacked as the one-dimensional spectra in Fig. 5a. In Fig. 5b, a fit example for the spectrum N8 to illustrate the possible deconvolution is presented.

As ^2H atoms are initially present only in heavy water as a constituent of the electrolyte, different water arrangements, hydrogen bonded (HB) complexes and surface hydroxides are expected to contribute to the starting ^2H NMR spectrum. The spectrum N1, which corresponds to an open voltage state (Fig. 5a), reveals the dominant peak at 4.6 ppm and smaller signals at 5.2, 8.0, 9.8, and 11.4 ppm. The narrow line at 4.6

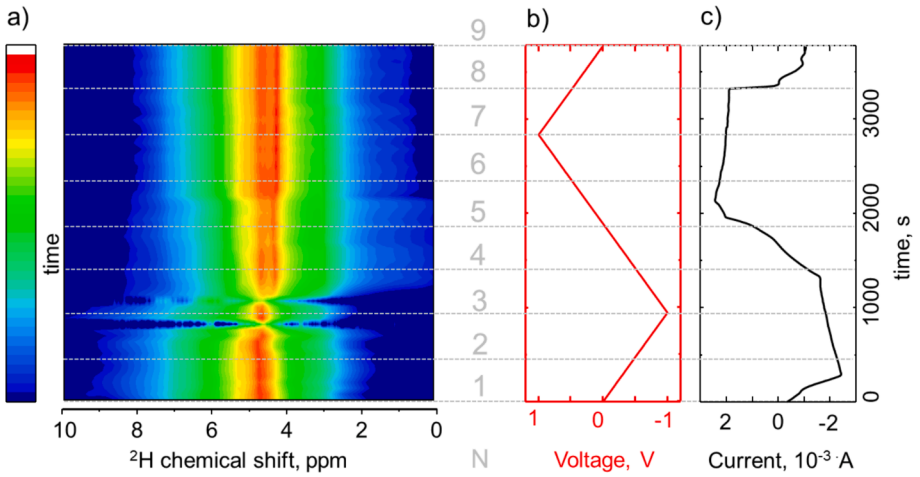

Fig. 4. (a) Two-dimensional ^{2}H NMR spectrum of electrochemical reduction of CO_2. (b) Voltage dependence and (c) current response as a function of time in chronoamperometry. N on the right of (a) indicates the number of the selected spectra presented in Fig. 5a.

ppm and the broader signal at 5.2 ppm are attributed to mobile water molecules in bulk electrolyte and less mobile water clusters at the electrode surface, respectively. The position of the latter is slightly shifted lowfield in respect to the bulk water signal due to proximity to the negatively charged Cu electrode surface. The intensity decrease of both water signals over the course of reaction evidences the water consumption for electrocatalysis. The downfield shifted signals at 9.8 and 11.4 ppm are a signature of strong hydrogen bonding (HB) characteristic of carboxyl groups [39]. Indeed, once potassium bicarbonate is dissolved in water, it dissociates completely to produce potassium cations K^+ and bicarbonate anions HCO_3^-. The ability of the latter to form HB complexes with heavy water molecules, such as OH-COO–-D-OH, and to produce dimers by hydrogen bonding with each other results in an appearance of the ^{2}H signals in this region [40–42]. The above discussed signals have been found in the spectra N1-N4, and then disappeared when the positive potential is applied. This evidences that such complexes are no longer present in the electrochemical system, and perhaps reacted to yield other reaction intermediates. This is accompanied by a reduction wave visible in Fig. 3c, when applied voltage achieves −0.3 V vs Pt. The signal at 8.0 ppm is typical for an intermediate HB strength and can be attributed to formate ions and their complexes with water molecules. Table 1 summarises the observed peaks and their assignment in the spectra N1 to N9.

In the spectrum N3 at a voltage of −1 V, a new poorly resolved signal at 2.3 ppm emerges. When applied potential increases, this signal evolves further and resolves into a sharp peak in the spectra N4-N9. Starting from the spectrum N4, the spectral profile in the central region changes revealing another new narrow peak at 4.0 ppm and the intense growth of the component at 5.2 ppm. The appearance of the peaks at 2.3 and 4.0 ppm visible in the spectra N4-N9 evidences the formation of new products in the course of electrochemical reaction. Among organic substances, several compounds are known to resonate around 2.3 ppm: acetone $CH_3-C(=O)-CH_3$(2.22 ppm), acetaldehyde CH_3-CHO (2.20 ppm), acetic acid CH_3-COOH (1.96 ppm) [43], acetylene $HC\equiv CH$ (2.01 ppm) [44]. Close to 4 ppm the resonances of methylene protons CH_2 in various acetylene compounds ($X-CH_2-C\equiv CH, X-CH_2-C\equiv CH_3$) have been found [44]. One can see that all signals emerged in the course of electroreduction arise from the deuterons bound to the carbon atoms, which are the part of carbon – carbon chain, and therefore are associated with multicarbon products. Thus, the in situ experiment in the present work clearly demonstrates generation of the reaction intermediates and products containing C–C bonds and thus indicates high selectivity to the C_{2+} hydrocarbon formation in this type of electrocatalytical system.

In the spectrum N7, which corresponds to the applied voltage of + 1 V, the minor signal at –1 ppm becomes visible and persists in the spectra N8 and N9 at + 0.5 and 0.0 V, respectively. The assignment of this signal is ambiguous, particularly, when not supported by other characterisation methods. The chemical shift value in this region is characteristic of metal hydroxides, which can be formed on the electrode surface. On the one hand, this signal can be assigned to isolated surface –CuOD groups not bound to water or other molecules. Then, its appearance in N7 can be explained by several reasons. Indeed, a continuous supply of heavy water molecules as the reaction proceeds results in their preferable adsorption on the electrode surface prompting the generation of abundant surface hydroxides. If the surface was initially protonated by –CuOH groups, the observed –CuOD groups can be produced as a result of isotope exchange with heavy water from electrolyte. Alternatively, hydroxyl radicals are known to be generated electrochemically from water at high anodic potentials [36]. On the catalytically active Cu electrode, preferential adsorption of highly reactive hydroxyl radicals can occur, which are further involved in the formation of hydrocarbon products through dimerization or protonation processes. Generally, observation of such a signal would be impossible under static NMR conditions considering the rigid nature of surface-immobilized species. On the other hand, the peak at −1 ppm could arise from hydrogen species in OH_x or CH_x groups chelated to paramagnetic Cu(II), which could give rise to ^{2}H NMR resonances across a broad chemical shift range.

The spectra N6, N7, N8 and N9 do not indicate significant changes, evidencing equilibrium in the electrochemical system. Fig. 4c demonstrates that the cathodic current corresponding to these spectra has been subsequently stabilized. It is worth to note, that in the ^{2}H spectra the fit component at 5.4 ppm can be distinguished, those linewidth is significantly smaller than that of the 5.2–ppm component. Based on literature data, the 5.4–ppm line is assigned to methane, which is known to a major product of CO_2 electroreduction reaction on a Cu electrode [45]. However, establishing conversion efficiency and pathway towards CH_4 production in the system under study is problematic due to poor spectral resolution.

It is notably, that when the applied potential approaches −1.0 V vs Pt (Fig. 4b), the 2D NMR spectrum demonstrates the nearly total intensity drop with the subsequent intensity recovery as voltage increases. Such phenomenon has been discussed in the previous section. Accordingly, in the present system, we can attribute this observation to the formation of paramagnetic radical reaction intermediates.

To sum up, in the in situ NMR experiment described above the products of CO_2 electroreduction have been observed. However, as mentioned above, a higher spectral resolution is required to achieve quantitative results and elucidate reaction mechanisms. Various

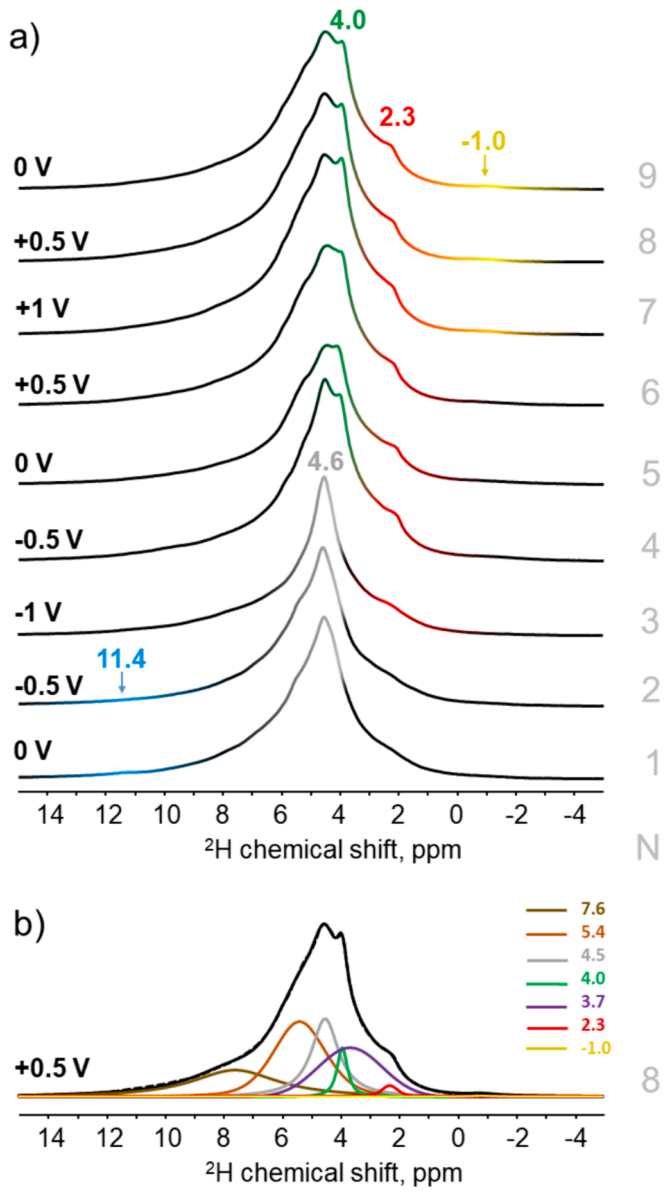

Fig. 5. (a) Selected ^{2}H NMR spectra from the voltage-dependent 2D ^{2}H NMR spectrum (see Fig. 4a). (b) Fit of the spectrum N8 at + 0.5 V. Chemical shift values of fit components (in ppm) are shown in Legend.

Table 1
The peaks observed in the spectra N1 to N9 and their assignment.

δ(^{2}H), ppm	Line width, ppm	Assignment
9.8–11.4	2.0–3.5	H-bonded carboxyl groups
8.0	1.5	H-bonded formate groups
5.4	2.1	Methane
5.2	4.5	immobilized water clusters on surface
4.6	1.2	mobile water molecules in bulk electrolyte
4.0	0.5	deuterons associated to C–C bonds
3.7	2.6	deuterons associated to C–C bonds
2.3	0.7	deuterons associated to C–C bonds
−1.0	1.0	surface metal hydroxides/OH_x or CH_x in Cu(II) chelates

approaches towards an enhanced resolution commonly employed in NMR spectroscopy include the application of decoupling techniques [46], varying the H/D concentration in aqueous solutions [47], and measurements of ^{13}C NMR spectra. These issues will be addressed in future studies to get a quantitative insight into electrochemical reduction of carbon dioxide.

4. Conclusion

In the present work we demonstrated the feasibility of in situ NMR using the customer built redox-flow cell. This cell is designed for hosting the electrochemical system, while continuous flow of liquid or gas is fed through the cell and electrical voltage is applied. The cell is to be placed into the NMR detection coil so that NMR signals can be measured at operando conditions enabling real time information on the dynamic structural changes and processes in the electrochemical system. The redox-flow cell described here is suitable for multiple uses, and allows detecting not only NMR signals from exhaust products, but also from those formed on the catalyst surface. The approach has been demonstrated using two case studies: electrodeposition of copper on an electrode and electrochemical reduction of carbon dioxide to valuable hydrocarbons. Analysis of the NMR spectra allowed to characterize the structural changes occurring once a copper film is formed on the electrode surface, in the former case study. Our results demonstrate the capability of in situ flow NMR for sstudying the properties of catalytical and active metal surfaces under varying chemical and electrical conditions. In the latter example, the existence of the multicarbon products produced as a result of electrocatalytical reaction is confirmed in the NMR spectra. In general, the reaction mechanism underlying this experiment can facilitate efficient and selective generation of valuable hydrocarbon products with the benefit of CO_2 conversion.

The data presented in this work are of great importance from both the methodological and application points of views, as it offers to exploit the distinct advantages of in situ NMR with respect to quantitative chemical species verification, and aims at innovative solutions to environmental and economic challenges.

CRediT authorship contribution statement

Anastasia Vyalikh: Writing – original draft, Validation, Investigation, Conceptualization. **Wolfram Münchgesang:** Writing – review & editing, Methodology, Investigation, Conceptualization. **Juan-Jesús Velasco-Vélez:** Writing – review & editing, Methodology.

Declaration of competing interest

The authors declare that they have no known competing financial interests or personal relationships that could have appeared to influence the work reported in this paper.

Data availability

Data will be made available on request.

Acknowledgement

We thank the German Federal Ministry of Education and Research (projects N° 05K14OFA and N° 05K14EWA) and the German Research Foundation (project La 655/23-1) for the financial support.

References

[1] A.R. Dahiru, A. Vuokila, M. Huuhtanen, Recent development in Power-to-X: Part I - A review on techno-economic analysis, J Energy Storage 56 (2022) 105861, https://doi.org/10.1016/j.est.2022.105861.
[2] R. Daiyan, I. MacGill, R. Amal, Opportunities and challenges for renewable power-to-X, ACS Energy Lett. 5 (2020) 3843–3847, https://doi.org/10.1021/acsenergylett.0c02249.
[3] C. van der Giesen, R. Kleijn, G.J. Kramer, Energy and climate impacts of producing synthetic hydrocarbon fuels from CO_2, Environ. Sci. Tech. 48 (2014) 7111–7121, https://doi.org/10.1021/es500191g.

[4] J. Artz, T.E. Müller, K. Thenert, J. Kleinekorte, R. Meys, A. Sternberg, A. Bardow, W. Leitner, Sustainable conversion of carbon dioxide: an integrated review of catalysis and life cycle assessment, Chem. Rev. 118 (2018) 434–504, https://doi.org/10.1021/acs.chemrev.7b00435.

[5] M. Rumayor, J. Fernández-González, A. Domínguez-Ramos, A. Irabien, Deep decarbonization of the cement sector: a prospective environmental assessment of CO_2 recycling to methanol, ACS Sustain. Chem. Eng. 10 (2022) 267–278, https://doi.org/10.1021/acssuschemeng.1c06118.

[6] N. Mac Dowell, P.S. Fennell, N. Shah, G.C. Maitland, The role of CO_2 capture and utilization in mitigating climate change, Nature Clim Change 7 (2017) 243–249, https://doi.org/10.1038/nclimate3231.

[7] Y. Zheng, A. Vasileff, X. Zhou, Y. Jiao, M. Jaroniec, S.-Z. Qiao, Understanding the roadmap for electrochemical reduction of CO_2 to multi-carbon oxygenates and hydrocarbons on copper-based catalysts, J. Am. Chem. Soc. 141 (2019) 7646–7659, https://doi.org/10.1021/jacs.9b02124.

[8] W. Deng, L. Zhang, L. Li, S. Chen, C. Hu, Z.-J. Zhao, T. Wang, J. Gong, Crucial role of surface hydroxyls on the activity and stability in electrochemical CO_2 reduction, J. Am. Chem. Soc. 141 (2019) 2911–2915, https://doi.org/10.1021/jacs.8b13786.

[9] K.P. Kuhl, E.R. Cave, D.N. Abram, T.F. Jaramillo, New insights into the electrochemical reduction of carbon dioxide on metallic copper surfaces, Energ. Environ. Sci. 5 (2012) 7050, https://doi.org/10.1039/C2EE21234J.

[10] H. Xiao, T. Cheng, W.A. Goddard, Atomistic mechanisms underlying selectivities in C_1 and C_2 products from electrochemical reduction of CO on Cu(111), J. Am. Chem. Soc. 139 (2017) 130–136, https://doi.org/10.1021/jacs.6b06846.

[11] C.S. Chen, J.H. Wan, B.S. Yeo, Electrochemical reduction of carbon dioxide to ethane using nanostructured Cu_2O-derived copper catalyst and palladium(II) chloride, J. Phys. Chem. C 119 (2015) 26875–26882, https://doi.org/10.1021/acs.jpcc.5b09144.

[12] C.D. Koolen, E. Oveisi, J. Zhang, M. Li, O.V. Safonova, J.K. Pedersen, J. Rossmeisl, W. Luo, A. Züttel, Low-temperature non-equilibrium synthesis of anisotropic multimetallic nanosurface alloys for electrochemical CO_2 reduction, Nat. Synth 3 (2024) 47–57, https://doi.org/10.1038/s44160-023-00387-3.

[13] D.M. Itkis, J.J. Velasco-Veléz, A. Knop-Gericke, A. Vyalikh, M.V. Avdeev, L. V. Yashina, Probing operating electrochemical interfaces by photons and neutrons, ChemElectroChem 2 (2015) 1427–1445, https://doi.org/10.1002/celc.201500155.

[14] J.J.A. Lozeman, P. Führer, W. Olthuis, M. Odijk, Spectroelectrochemistry, the future of visualizing electrode processes by hyphenating electrochemistry with spectroscopic techniques, Analyst 145 (2020) 2482–2509, https://doi.org/10.1039/c9an02105a.

[15] M. Pietrzak, S. Jopa, A. Mames, M. Urbańczyk, M. Woźny, T. Ratajczyk, Recent progress in liquid state electrochemistry coupled with NMR spectroscopy, ChemElectroChem 8 (2021) 4181–4198, https://doi.org/10.1002/celc.202100724.

[16] L. Huang, E.G. Sorte, S.-G. Sun, Y.Y.J. Tong, A straightforward implementation of in situ solution electrochemical ^{13}C NMR spectroscopy for studying reactions on commercial electrocatalysts: ethanol oxidation, Chem. Commun. 51 (2015) 8086–8088, https://doi.org/10.1039/C5CC00862J.

[17] S. Klod, F. Ziegs, L. Dunsch, In situ NMR spectroelectrochemistry of higher sensitivity by large scale electrodes, Anal. Chem. 81 (2009) 10262–10267, https://doi.org/10.1021/ac901641m.

[18] J.-M. Tarascon, A.S. Gozdz, C. Schmutz, F. Shokoohi, P.C. Warren, Performance of Bellcore's plastic rechargeable Li-ion batteries, Solid State Ion. 86–88 (1996) 49–54, https://doi.org/10.1016/0167-2738(96)00330-X.

[19] J.B. Richter, C. Eßbach, I. Senkovska, S. Kaskel, E. Brunner, Quantitative in situ ^{13}C NMR studies of the electro-catalytic oxidation of ethanol, Chem. Commun. 55 (2019) 6042–6045, https://doi.org/10.1039/c9cc02660f#.

[20] P. Da Ferreira Silva, T. Santana Ribeiro, B. Ferreira Gomes, G. Da Tiago Dos Santos Tavares Silva, C.M. Silva Lobo, M. Carmo, C. Ribeiro, R. Bernardes Filho, C. Roth, L.A. Colnago, Miniaturized Carbon Fiber Paper Electrodes for In Situ High Resolution NMR Analyses, Anal Chem 94 (2022) 15223–15230. https://doi.org/10.1021/acs.analchem.2c02058.

[21] M. Liu, Z.-R. Ni, H.-J. Sun, S.-H. Cao, Z. Chen, In situ real-time quantitative determination in electrochemical nuclear magnetic resonance spectroscopy, Sensors (Basel) 22 (2022) 282, https://doi.org/10.3390/s22010282.

[22] R.Y. Hwang, O.H. Han, Flow NMR system development for real-time in situ multiple detection of direct methanol fuel cell exhausts, Electrochem. Commun. 148 (2023) 107417, https://doi.org/10.1016/j.elecom.2022.107417.

[23] O. Pecher, A. Vyalikh, C.P. Grey, Challenges and new opportunities of in situ NMR characterization of electrochemical processes, AIP Conf. Proc. 1765 (2016) 20011, https://doi.org/10.1063/1.4961903.

[24] A. Vyalikh, T. Köhler, T. Zakharchenko, D.M. Itkis, A. Krajnc, G. Mali, Magnetic resonance spectroscopy approaches for electrochemical research, Phys. Sci. Rev. 3 (2018), https://doi.org/10.1515/psr-2017-0155.

[25] G.C. Carter, L.H. Bennett, D.J. Kahan, Metallic shifts in NMR, Part 1, in: B. Chalmers, J.W. Christian, T.B. Massalski (Eds.), Progress in Materials Science, Vol. 20, Pergamon Press, 1977.

[26] J.-J. Velasco-Vélez, K. Skorupska, E. Frei, Y.-C. Huang, C.-L. Dong, B.-J. Su, C.-J. Hsu, H.-Y. Chou, J.-M. Chen, P. Strasser, R. Schlögl, A. Knop-Gericke, C.-H. Chuang, The electro-deposition/dissolution of $CuSO_4$ aqueous electrolyte investigated by in situ Soft X-ray absorption spectroscopy, J. Phys. Chem. B 122 (2018) 780–787, https://doi.org/10.1021/acs.jpcb.7b06728.

[27] J.-J. Velasco-Veléz, R.V. Mom, L.-E. Sandoval-Diaz, L.J. Falling, C.-H. Chuang, D. Gao, T.E. Jones, Q. Zhu, R. Arrigo, B. Roldan Cuenya, A. Knop-Gericke, T. Lunkenbein, R. Schlögl, Revealing the active phase of copper during the electroreduction of CO_2 in aqueous electrolyte by correlating in situ X-ray spectroscopy and in situ electron microscopy, ACS Energy Lett. 5 (2020) 2106–2111, https://doi.org/10.1021/acsenergylett.0c00802.

[28] D. Massiot, F. Fayon, M. Capron, I. King, S. Le Calvé, B. Alonso, J.-O. Durand, B. Bujoli, Z. Gan, G. Hoatson, Modelling one- and two-dimensional solid-state NMR spectra, Magn. Reson. Chem. 40 (2002) 70–76, https://doi.org/10.1002/mrc.984.

[29] J.-J. Velasco-Vélez, T. Jones, D. Gao, E. Carbonio, R. Arrigo, C.-J. Hsu, Y.-C. Huang, C.-L. Dong, J.-M. Chen, J.-F. Lee, P. Strasser, B. Roldan Cuenya, R. Schlögl, A. Knop-Gericke, C.-H. Chuang, The role of the copper oxidation state in the electrocatalytic reduction of CO_2 into valuable hydrocarbons, ACS Sustain. Chem. Eng. 7 (2019) 1485–1492, https://doi.org/10.1021/acssuschemeng.8b05106.

[30] B. Endrődi, G. Bencsik, F. Darvas, R. Jones, K. Rajeshwar, C. Janáky, Continuous-flow electroreduction of carbon dioxide, Prog. Energy Combust. Sci. 62 (2017) 133–154, https://doi.org/10.1016/j.pecs.2017.05.005.

[31] A.A. Permyakova, J. Herranz, M. El Kazzi, J.S. Diercks, M. Povia, L.R. Mangani, M. Horisberger, A. Pătru, T.J. Schmidt, On the oxidation state of Cu_2O upon electrochemical CO_2 reduction: An XPS Study, ChemPhysChem 20 (2019) 3120–3127, https://doi.org/10.1002/cphc.201900468.

[32] J.-J. Velasco-Vélez, J. Poon, D. Gao, C.-H. Chuang, A. Bergmann, T.E. Jones, S.-C. Haw, J.-M. Chen, E. Carbonio, R.V. Mom, D. Ivanov, R. Arrigo, B.R. Cuenya, A. Knop-Gericke, R. Schlögl, Cationic copper species stabilized by zinc during the electrocatalytic reduction of CO_2 revealed by In Situ X-Ray spectroscopy, Adv. Sustain. Syst. 7 (2023) 2200453, https://doi.org/10.1002/adsu.202200453.

[33] B. Schmid, C. Reller, S. Neubauer, M. Fleischer, R. Dorta, G. Schmid, Reactivity of copper electrodes towards functional groups and small molecules in the context of CO_2 electro-reductions, Catalysts 7 (2017) 161, https://doi.org/10.3390/catal7050161.

[34] J. Lee, Y. Tak, Electrocatalytic activity of Cu electrode in electroreduction of CO_2, Electrochim. Acta 46 (2001) 3015–3022, https://doi.org/10.1016/S0013-4686(01)00527-8.

[35] Y. Hori, K. Kikuchi, S. Suzuki, Production of CO and CH_4 in electrchemical reduction of CO_2 at metal electrodes in aqueous hydrogencarbonate solution, Chem. Lett. 14 (1985) 1695–1698, https://doi.org/10.1246/cl.1985.1695.

[36] E. Braxton, D.J. Fox, B.G. Breeze, J.J. Tully, K.J. Levey, M.E. Newton, J. V. Macpherson, Electron paramagnetic resonance for the detection of electrochemically generated hydroxyl radicals: issues associated with electrochemical oxidation of the spin trap, ACS Meas. Sci. Au 3 (2023) 21–31, https://doi.org/10.1021/acsmeasuresciau.2c00049.

[37] T. Shimizu, T. Matsumoto, A. Goto, T.V. Chandrasekhar Rao, K. Yoshimura, K. Kosuge, Spin susceptibility and superexchange interaction in the antiferromagnet CuO, Phys. Rev. B 68 (2003) 224433, https://doi.org/10.1103/PhysRevB.68.224433.

[38] G.E. Peterson, in: Charge Distributions in Ionic Crystals from the NMR and NQR of Na and Cu, Resonance, Springer, New York, NY, 1970, pp. 41–61.

[39] L.L. Kimtys, V.J. Balevičius, Self-association of carboxylic acids as studied by ^1H NMR spectroscopy, Adv. Mol. Relax. Interact. Process. 15 (1979) 151–161, https://doi.org/10.1016/0378-4487(79)80029-1.

[40] P.M. Tolstoy, P. Schah-Mohammedi, S.N. Smirnov, N.S. Golubev, G.S. Denisov, H.-H. Limbach, Characterization of fluxional hydrogen-bonded complexes of acetic acid and acetate by NMR: geometries and isotope and solvent effects, J. Am. Chem. Soc. 126 (2004) 5621–5634, https://doi.org/10.1021/ja039280j.

[41] A. Vyalikh, T. Emmler, B. Grünberg, Y. Xu, I. Shenderovich, G.H. Findenegg, H.-H. Limbach, G. Buntkowsky, Hydrogen Bonding of Water Confined in Controlled-Pore Glass 10–75 Studied by ^1H-Solid State NMR, Z. Phys. Chem. 221 (2007) 155–168, https://doi.org/10.1524/zpch.2007.221.1.155.

[42] G. Buntkowsky, H. Breitzke, A. Adamczyk, F. Roelofs, T. Emmler, E. Gedat, B. Grünberg, Y. Xu, H.-H. Limbach, I. Shenderovich, A. Vyalikh, G. Findenegg, Structural and dynamical properties of guest molecules confined in mesoporous silica materials revealed by NMR, Phys Chem Chem Phys 9 (2007) 4843–4853, https://doi.org/10.1039/B707322D.

[43] National Institutes of Health, PubChem: National Library of Medicine 8600 Rockville Pike, Bethesda, MD 20894. https://pubchem.ncbi.nlm.nih.gov/.

[44] Hans Reich, Hans Reich's Collection. NMR Spectroscopy. https://organicchemistrydata.org/hansreich/resources/nmr.

[45] Z. Han, R. Kortlever, H.-Y. Chen, J.C. Peters, T. Agapie, CO_2 Reduction Selective for C≥2 products on polycrystalline copper with N-Substituted pyridinium additives, ACS Cent. Sci. 3 (2017) 853–859, https://doi.org/10.1021/acscentsci.7b00180.

[46] R. Freeman, E. Kupče, Decoupling: theory and practice I, Current Methods and Recent Concepts, NMR Biomed. 10 (1997) 372–380, https://doi.org/10.1002/(SICI)1099-1492(199712)10:8<372:AID-NBM478>3.0.CO;2-Z.

[47] H.-H. Limbach, Dynamic NMR spectroscopy in the presence of kinetic hydrogen/deuterium isotope effects, in: NMR Basic Principles and Progress, Vol. 23, Springer Verlag, Berlin, Heidelberg, 1990, pp. 63–164.